

## Unusual magnetism in templated NiS nanoparticles

This article has been downloaded from IOPscience. Please scroll down to see the full text article.

2010 J. Phys.: Condens. Matter 22 076001

(<http://iopscience.iop.org/0953-8984/22/7/076001>)

View [the table of contents for this issue](#), or go to the [journal homepage](#) for more

Download details:

IP Address: 129.252.86.83

The article was downloaded on 30/05/2010 at 07:12

Please note that [terms and conditions apply](#).

# Unusual magnetism in templated NiS nanoparticles

Louise Barry<sup>1</sup>, Justin D Holmes<sup>1,2</sup>, David J Otway<sup>1</sup>,  
Mark P Copley<sup>1</sup>, Olga Kazakova<sup>3</sup> and Michael A Morris<sup>1,2,4</sup>

<sup>1</sup> Department of Chemistry, University College Cork, Cork, Republic of Ireland

<sup>2</sup> Centre for Research on Adaptive Nanostructures and Nanodevices (CRANN),  
Trinity College Dublin, Dublin 2, Republic of Ireland

<sup>3</sup> National Physical Laboratory, Teddington, UK

E-mail: [m.morris@ucc.ie](mailto:m.morris@ucc.ie)

Received 14 August 2009, in final form 10 December 2009

Published 29 January 2010

Online at [stacks.iop.org/JPhysCM/22/076001](http://stacks.iop.org/JPhysCM/22/076001)

## Abstract

Nanostructured NiS was prepared by inclusion into anodic alumina templates. The resultant particles were found to be stoichiometric and highly crystalline. The particles displayed small particle superparamagnetism, and a low temperature (at 48 K ( $T_{sg}$ )) spin-freezing phenomenon (a spin-glass) and higher temperature (170 K) thermal blocking of small particle magnetic moment fluctuations were both observed for the first time for a sulfide material. Very unusually, these NiS materials are quite distinct from antiferromagnetic nanoparticulate sulfide materials, as they display a high temperature ferromagnetic-like phase. The saturation magnetization, the remanent magnetization, the coercivity and the ferromagnetic mass susceptibility were measured as 0.58 emu g<sup>-1</sup> (at 100 K), 0.19 emu g<sup>-1</sup>, 219.5 Oe (at 170 K) and  $\sim 900 \times 10^{-6}$  emu Oe<sup>-1</sup> g<sup>-1</sup> respectively and these are consistent with a moderately strong ferromagnetism. The materials had an unexpectedly high Curie temperature of 390 K. The decrease of the saturation magnetization value at 30 K suggests that the ferromagnetic response is a surface phenomenon and the high coercivity of the paramagnetic component well above  $T_{sg}$  suggests that the core can be described as superparamagnetic.

## 1. Introduction

In this paper we report unusual magnetic properties of NiS nanoparticles and suggest that NiS may have technological importance as a ferromagnetic semiconductor. Metal sulfides can have considerable advantages compared to metals and oxides, combining mechanical and thermal robustness with additional chemical stability particularly in hydrothermal conditions and, therefore, can be easier to prepare in non-aggregated nanoparticulate form. Many of the metal sulfides show interesting electrical and magnetic properties (essentially because of broad sulfur bands) with a wide range of semiconducting and metallic compounds known [1]. The magnetic properties of the spinel ferrimagnetic semiconductors [2] and mineral phases such as pyrrhotite [3] have attracted interest for device technologies. EuS is a low temperature ferromagnetic sulfide that has attracted interest as a possible spin filter [4]. However, apart from the few

established sulfide ferrimagnetics [1] the sulfides only show interesting magnetic properties at very low temperatures where spin-glass and blocking effects could be important and where the dynamic nature of these phenomena would, by necessity, lead to irreproducibility in performance [5]. One means of evolving a new class of useful sulfide magnetic materials is to use size control to generate superparamagnetism and ferromagnetism in classically antiferromagnetic materials [6]. This is common for metallic and oxide systems but has only been sparingly applied for sulfide systems, particularly so for non-ferrous systems where bacteria-mediated synthesis has been used [7].

Recently, we observed an unusual low temperature blocking effect in MnS nanoparticles [8]. Here, for the first time we report a nanoscale sulfide system that demonstrates high temperature ferromagnetism together with low temperature superparamagnetism and associated blocking and spin-glass effects. The ferromagnetism is of moderate strength such that lightly ground NiS loaded membranes

<sup>4</sup> Author to whom any correspondence should be addressed.

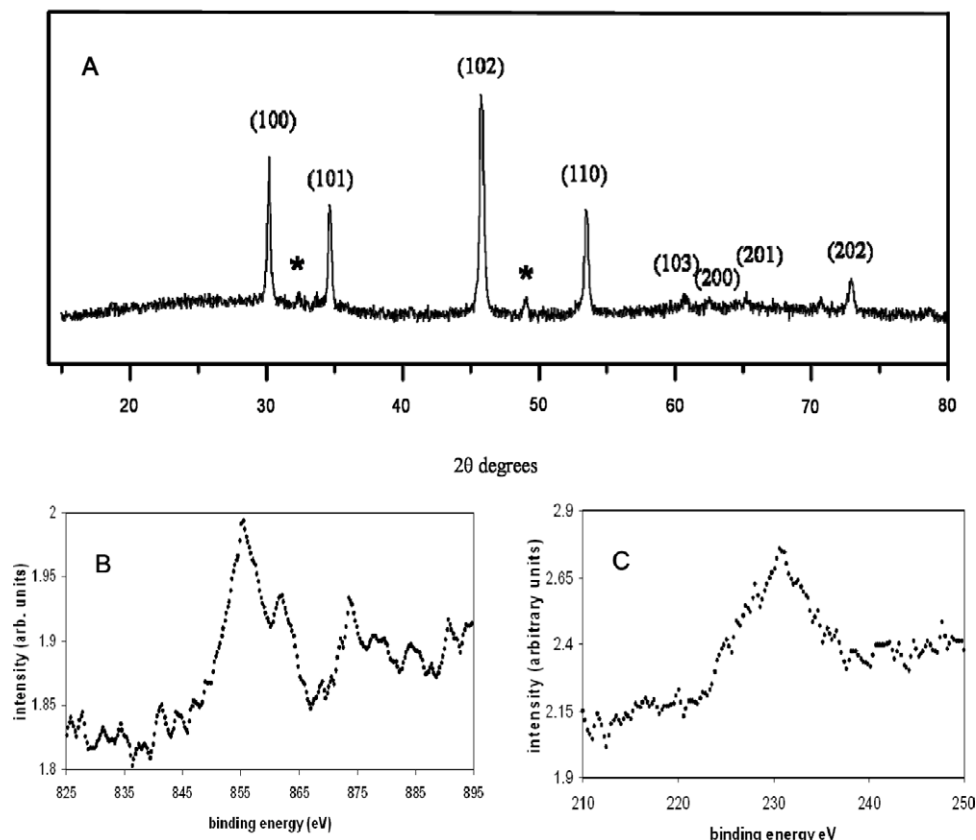


**Figure 1.** (A) XRD data from the NiS filled AAO templates. (B) and (C) Ni 2p and S 3s photoelectron spectra from the NiS-AAO.

were strongly attracted to a magnet. Ferromagnetism is unexpected as bulk  $\alpha$ -NiS material is known to have a low temperature antiferromagnetic semiconductor to a paramagnetic metallic phase transition at 263 K [9]. Recent studies of nanoparticulate  $\alpha$ -NiS suggest strong size effects and paramagnetic behaviour [10]. A very weak ferromagnetic behaviour was also observed (saturation magnetization of  $1.2 \times 10^{-4}$  emu g $^{-1}$  [10]) and the data are consistent with superparamagnetism.

## 2. Experimental details

Aggregated nanoparticles of  $\alpha$ -NiS were formed in the AAO pores by inclusion and subsequent decomposition of a novel nickel ethyl xanthate single source precursor within an anodic alumina (AAO) membrane template (Whatman International Ltd, Anodisc, nominal pore diameter = 0.2  $\mu$ m). The xanthate precursor (nickel ethylxanthate (Ni[(S<sub>2</sub>COEt)<sub>2</sub>]TMEDA) was synthesized as manganese precursor described earlier [8]. The precursor was decomposed in supercritical CO<sub>2</sub> at 450 °C, at 4000 psi for 90 min within a steel cell containing the AAO membrane [11]. The recovered membrane was washed and polished to remove surface materials. The sulfide formed has an apparent stoichiometry of NiS as indicated by x-ray fluorescence spectroscopy (XRF, Siemens SX Pico) and energy dispersive x-ray analysis (EDAX, Oxford Instruments INCA). Thermal analysis during decomposition of the precursor also indicated the formation of stoichiometric

NiS. Besides Ni, S, Al, O no other peaks were visible in EDAX or XRF indicating contamination of the sample was negligible. Stoichiometry, chemical composition and structure were further confirmed by powder x-ray diffraction (XRD, PANalytical MRD) and x-ray photoelectron spectroscopy (XPS, Vacuum Science Workshop). Transmission electron microscopy data were collected on a JEOL JEM-200FX operating at 200 kV. Magnetization measurements were performed using a commercial SQUID (superconductor quantum interference device) magnetometer (MPMS XL, Quantum Design).

## 3. Results

Figure 1(A) shows a typical diffractogram that can be readily indexed to the hexagonal structure of  $\alpha$ -NiS (JCPDS, No. 02-1280). Two minor features (\*) can be indexed to the (300) and (131) planes of rhombohedral millerite  $\beta$ -NiS (JCPDS, No. 86-2280). No peaks from impurities such as Ni, NiO<sub>x</sub> and non-stoichiometric nickel sulfide phases were detected. Least squares analysis of the diffraction pattern indicates unit cell parameters of  $a_0 = b_0 = 0.3415$  and  $c_0 = 0.5351$  nm. The measured cell parameters are consistent with stoichiometric  $\alpha$ -NiS as the  $c_0$  value is particularly sensitive to non-stoichiometry [12]. Ni 2p<sub>3/2</sub> and S 3s XPS features are shown in figures 1(B) and (C). The peak area analysis gives a Ni:S atomic ratio of 1.0 ( $\pm 0.025$ ) consistent with XRD data. The shape and position (855.3 eV) of the Ni 2p peaks are

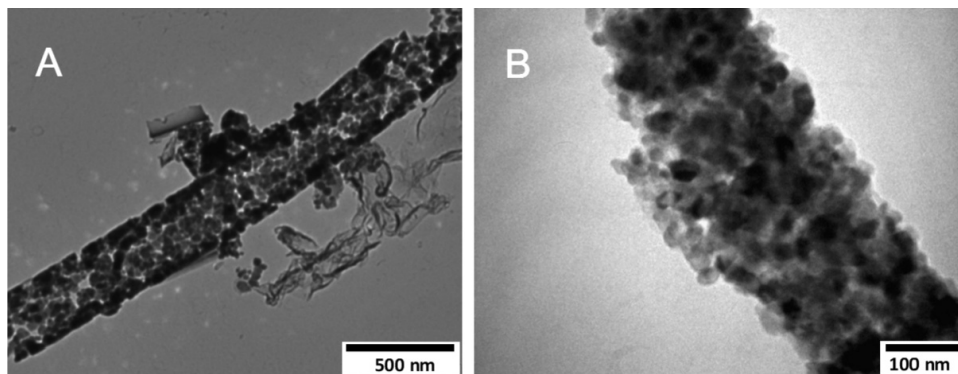


**Figure 2.** TEM images of typical NiS nanostructures obtained from the SCF method.

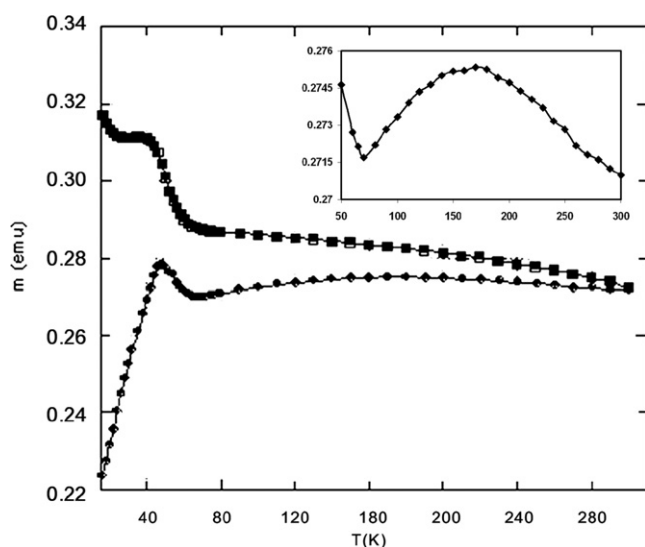


**Figure 3.** ● Zero-field-cooled (ZFC) and ■ field-cooled (FC) magnetic moment versus temperature plots for a NiS-AAO sample at an external magnetic field of 500 Oe. The inset is a magnification of the moment measured in ZFC conditions.

entirely consistent with  $\alpha$ -NiS as are the S 3s (230.9 eV) and S 2p (161.5 eV) features [13].

TEM images reveal the nanoparticulate nature of the templated included material. Figure 2(A) shows an image of NiS nanowire-like moieties released by oxide dissolution of the alumina. Figure 2(B) shows the central part of a nanowire. The wires are made up of nanoparticles around 20–25 nm in diameter. XRD would suggest a larger particle size but this is because quite dense NiS is formed as a uniform thickness coating ( $\sim 25$  nm) at the pore wall.

Temperature dependencies of magnetization of the  $\alpha$ -NiS filled membranes as measured at  $H = 500$  Oe are shown in figure 3 for zero-field-cooled (ZFC) and field-cooled (FC) conditions. These curves show temperature dependence atypical of either a simple paramagnetic or antiferromagnetic material and are strongly reminiscent of data collected for NiO nanoparticles [14] except for the presence of a strong ferromagnetic-like component with high Curie temperature ( $T_C$ ). At around 300 K bifurcation of the  $M_{ZFC}$  and  $M_{FC}$  curves can be observed. The separation of the curves may

reflect low temperature blocking effects [15] (see below) or strong interparticle interactions that lead to an interaction field effect greater than the applied field [16]. Interparticle interactions do play an important role in this system because if the alumina is dissolved in KOH to leave a only a distribution of small particles, the magnetic effects seen for the membrane sample were much reduced. The magnetization present at 300 K indicates a permanent magnetic moment. At lower temperatures the  $M_{ZFC}$  and  $M_{FC}$  curves are not reflective of simple paramagnetism or superparamagnetism. In particular, on the  $M_{ZFC}$  curve two distinct maxima can be observed at  $T_{sg} = 48$  K (a well-resolved peak) and at  $T_b = 170$  K (a broad and weak maximum). The feature at  $T_b$  can be better resolved on the background subtracted data (figure 3, inset). In NiO these features have been explained in terms of a low temperature spin-freezing phenomenon (a spin-glass) and a higher temperature feature which represents thermal blocking of small particle magnetic moment fluctuations and can be described by classic Néel superparamagnetism [17]. The broadness of the 170 K feature is probably associated with the distribution of particle sizes (which can also be seen in the TEM images) within the sample (resulting in an anisotropic distribution of activation energies) and the relatively high blocking temperature ( $T_b$ ) is related to strong interparticle interactions [18]. Modelling of amorphous metal alloy nanoparticles (systems where these effects were first observed) [15] suggest that the blocking is associated with the particle core whilst the spin-freezing is related to a shell of surface spins [15, 19, 20]. The freezing of spin-states is also associated with a plateau region of  $M_{FC}$  curves [16, 21–23] and this can be clearly seen in figure 3. Bulk NiS is an antiferromagnetic material and, by analogy with NiO, one might expect similar behaviour. To our knowledge this is the first time the combination of spin-glass and core blocking have been observed in a sulfide material.

What differentiates the NiS from the NiO and other bulk antiferromagnetic nanoparticulate sulfide materials is the presence of a high temperature ferromagnetic-like phase. This is explored further in  $M$  versus  $H$  data shown at several temperatures in figure 4. No magnetization saturation has been observed in magnetic fields up to 6 kOe in the whole temperature range indicating the presence of a paramagnetic component. At all recorded temperatures the

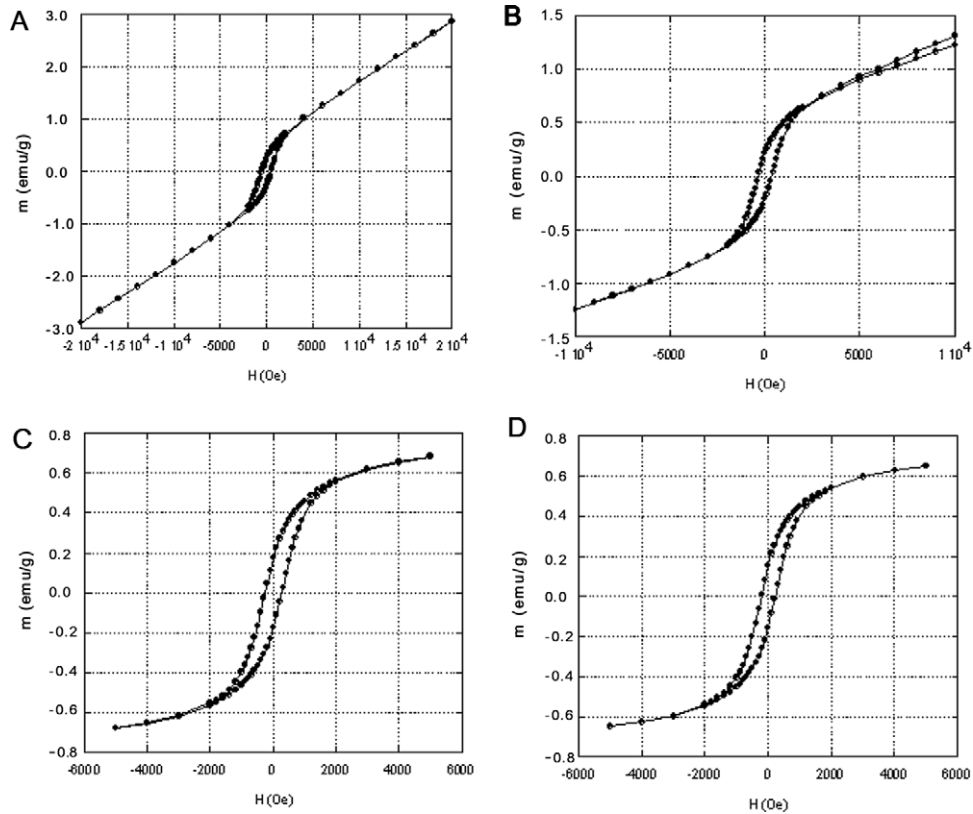


Figure 4. Magnetic hysteresis loops of NiS loaded AAO membrane at (A) 10, (B) 30, (C) 70 and (D) 170 K.

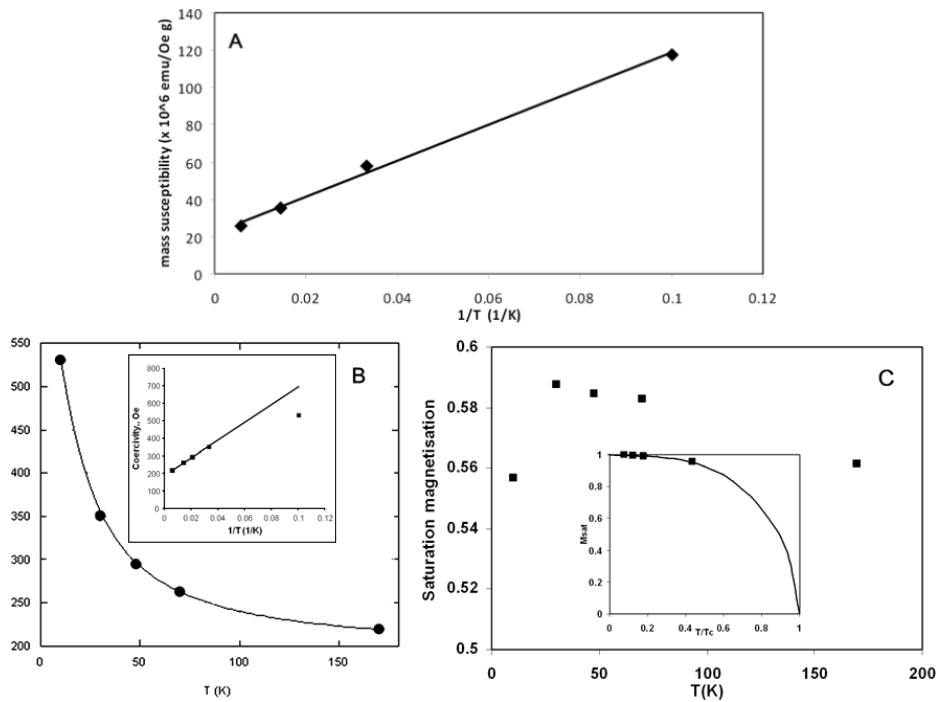


Figure 5. (A) Paramagnetic susceptibility versus reciprocal temperature. (B) and (C) plots of coercivity and saturation magnetization ( $\text{emu g}^{-1}$ ) versus temperature respectively. Lines in A and B are guides for the eye. The line in the inset to (C) is a fit to data (see text).

curve reflects a mixture of linear paramagnetic-like and hysteretic ferromagnetic-like contributions (above 70 K). The ferromagnetic component displays hysteresis which

is symmetrical about zero field. The paramagnetic and ferromagnetic components can be separated by subtraction of a linear component from slopes at relatively high field. Thus, a



paramagnetic mass susceptibility measured at high field ( $\chi_{\text{HF}}$ ) and a saturation magnetization ( $M_{\text{S}}$ ) can be derived.  $\chi_{\text{HF}}$  plots versus reciprocal temperature (figure 5(A)) are consistent with the Curie law proving paramagnetism in these particles. The value of  $\chi_{\text{HF}}$  at 10 K,  $118 \times 10^{-6} \text{ emu Oe}^{-1} \text{ g}^{-1}$  is significantly larger than reported in other NiS nanoparticles (about  $0.1 \times 10^{-6}$  [10],  $30 \times 10^{-6}$  [24],  $50 \times 10^{-6}$  [25]  $\text{emu Oe}^{-1} \text{ g}^{-1}$ ).

The well-defined hysteresis in the  $M$ – $H$  curves is present at all temperatures up to 170 K and shows no shifts or irregularities through the temperature range studied indicating the absence of exchange bias effects [26]. The lack of any detectable exchange bias effect suggests that the majority of the sample is not antiferromagnetic and the particles are below the superparamagnetic size limit [15, 16]. Derived coercivity values ( $H_{\text{c}}$ ) and saturation magnetization versus temperature are plotted in figure 5(B) and (C). The observed saturation, the remanent magnetization ( $M_{\text{r}} = 0.19 \text{ emu g}^{-1}$ ), the relatively large value of  $H_{\text{c}}$  even at  $T_{\text{b}}$  ( $H_{\text{c}}$  at 170 K = 219.5 Oe), the invariance of  $M_{\text{S}}$  with temperature and a value of ferromagnetic mass susceptibility ( $\sim 900 \times 10^{-6} \text{ emu Oe}^{-1} \text{ g}^{-1}$ ) all suggest that the particles are ferromagnetic. Plots of  $M_{\text{S}}$  versus temperature (figure 5(C)) show a decrease in  $M_{\text{S}}$  below 30 K that can be associated with the spin-glass transition and implies that the ferromagnetism is a surface effect. Fitting of the data from 30 to 170 K with a Brillouin function ( $S = 1$ ) suggests a  $T_{\text{c}}$  around 390 K (figure 5(C)). We note that this fit is based on only a few points and should be viewed as an estimate only with a possible error of around  $\pm 75$  K. However, this is substantially higher than might be expected (see below). The marked increase in  $H_{\text{c}}$  below 170 K is consistent with the observed blocking temperature, since below  $T_{\text{b}}$  the paramagnetic particles are constrained from alignment in the field. Plotting  $H_{\text{c}}$  versus  $1/T$  (figure 5(B) inset) allows determination of the high temperature limit of the coercivity (=190 Oe) and this indicates the paramagnetic contribution to the coercivity at 170 K ( $T_{\text{b}}$ ) is 29 Oe and this is consistent with the assignment of a superparamagnetic contribution as  $H_{\text{c}}$  and  $H_{\text{r}}$  should decrease to zero above the blocking temperature [6].

#### 4. Discussion

Room temperature ferro/ferrimagnetism combined with superparamagnetism in nanoparticles has been observed in, e.g., Pd [27], Ge [28] and NiO [12] amongst others. Very weak low temperature ferromagnetism/paramagnetism has been observed in  $\alpha$ -NiS platelets [10] and  $\beta$ -NiS tubes [25] but blocking and spin trapping have not been reported. There has been one report of moderate ferromagnetism in  $\alpha$ -NiS nanoparticles with a  $M_{\text{r}}$  value of 0.11  $\text{emu g}^{-1}$  (low temperatures were not investigated) but the sulfide was produced in strongly reducing conditions and the presence of additional peaks in XRD profiles suggests that the presence of non-stoichiometric or metal phases can not be ruled out. It is generally accepted that spin-glass (surface shell) combined with blocking effects (core) can be explained by a core–shell particle model. The decrease of the  $M_{\text{S}}$  value at 30 K suggests that the ferromagnetic response

is a surface phenomenon and the high coercivity of the paramagnetic component well above  $T_{\text{sg}}$  suggests the core can be described as superparamagnetic. This is qualitatively similar to the work reported on Pd nanoparticles [27] and indeed  $H_{\text{c}}$ ,  $M_{\text{r}}$ ,  $M_{\text{S}}$  and the susceptibility of the ferromagnetism reported here is quite close to the Pd values.

The origin of magnetism in these materials is still poorly understood. Bulk NiS does exhibit paramagnetism in the bulk and above a transition temperature it changes from an antiferromagnetic semiconductor into paramagnetic metallic state [29]. The phase transition temperature ( $T_{\text{I}}$ ) is reduced by pressure and nickel deficiency [10] but the presence of blocking and spin effects would suggest that the paramagnetism observed here is properly described as superparamagnetism arising from uncompensated spins in small particles. Note that all the magnetic data were collected below the  $T_{\text{I}}$  (263 K) of stoichiometric  $\alpha$ -NiS. The surface ferromagnetism is less easily described and may originate from surface atom coordination changes, band structure or lattice changes. The band structure of NiS is not well understood but is clear that lowest unoccupied bands and highest filled bands are in close proximity [30] and evidence for Ni 3d–S 2p hybridization has been reported [31]. Surface changes in this band structure might allow uncompensated surface spins to develop. Of course, these are relatively large particles and one might expect surface effects to be small. However the system is complex and surface effects may originate from (A) interparticle spacing and related effects or (2) although the ratio of surface atoms to bulk atoms is relatively small it is probably better to think about surface unit cells and bulk unit cells, and this ratio is much larger.

In conclusion, evidence for unusual magnetism in NiS particles is given. Whilst of scientific interest it may also be of significant technological importance because of the possibility of creating room temperature magnetic semiconductors for use in spintronics applications [32].

#### Acknowledgments

IRCSET are gratefully acknowledged for student support for Louise Barry. Science Foundation Ireland are thanked for project support through the Principal Investigator Grant: Structurally and Size-Controlled Nanowires, into 3D Architectures and Construction of Prototype Circuitry' (03/IN3/I375). We also thank Professor T R Spalding for helpful suggestions through the course of this work.

#### References

- [1] Pearce C I, Patrick R A D and Vaughan D J 2006 *Rev. Mineral. Geochem.* **61** 127
- [2] Vaqueiro P, Sommer S and Powell A V 2000 *J. Mater. Chem.* **10** 2381
- [3] Takayama T and Takagi H 2006 *Appl. Phys. Lett.* **88** 012512
- [4] Metzke R and Nolting W 1998 *Phys. Rev. B* **58** 8579
- [5] Campbell I A, Hammann J, Kawamura H, McKenzie R H, Nordblad P, Orbach R and Takayama H 1998 *J. Magn. Magn. Mater.* **177–181** 63

- [6] Lu A-H, Salabas E L and Schüth F 2007 *Angew. Chem. Int. Edn* **46** 1222
- [7] Bharde A A, Parikh R Y, Baidakova M, Jouen S, Hannoyer B, Enoki T, Prasad B L V, Shouche Y S, Ogale S and Sastry M 2008 *Langmuir* **24** 5787
- [8] Barry L, Copley M, Holmes J D, Otway D J, Kazakova O and Morris M A 2007 *J. Solid State Chem.* **180** 2443
- [9] Sparks J T and Komoto T 1968 *Rev. Mod. Phys.* **40** 752
- [10] Zhang H T, Wu G and Chen X H 2005 *Mater. Lett.* **59** 3728
- [11] More complete experimental set-up details are given in e.g. Xu J, Zhang W, Morris M A and Holmes J D 2007 *Mater. Chem. Phys.* **104** 50
- [12] Borisenko D N, Dubinov A E, Kolesnikov N N, Kudasov Y B, Kulakov M P and Shalynin A I 2003 *J. Cryst. Growth* **253** 307
- [13] Wagner C D 1979 *Handbook of X-Ray Photoelectron Spectroscopy* (Minnesota: Perkin-Elmer)  
Briggs D and Seah M P 1993 *Practical Surface Analysis* 2nd edn (New York: Wiley)
- [14] Thota S and Kumar J 2007 *J. Phys. Chem. Solids* **68** 1951
- [15] De Biasi E, Ramos C A, Zysler R D and Romero H 2002 *Phys. Rev. B* **65** 144416
- [16] Gajbhiye N S and Bhattacharyya S 2004 *Phys. Status Solidi* **12** 3764
- [17] Néel L 1961 *J. Phys. Soc. Japan* **17** (Suppl. B1) 676
- [18] Néel L 1949 *Ann. Geophys.* **5** 99
- [19] Mydosh J A 1993 *Spin Glasses* (London: Taylor and Francis)
- [20] Zysler R D, Ramos C A, De Biasi E, Romero H, Ortega A and Fiorani D 2000 *J. Magn. Magn. Mater.* **221** 37
- [21] Romero H, Ortega A, Zysler R D, Ramos C, De Biasi E and Fiorani D 2000 *Phys. Status Solidi* **220** 401
- [22] Shim H, Dutta P, Seehra M S and Bonevich J 2008 *Solid State Commun.* **145** 192
- [23] Zysler R D, Vasquez Mansilla M and Fiorani D 2005 *Phys. Rev. B* **72** 32409
- [24] Wang W, Wang S-Y, Gao Y-L, Wang K-Y and Liu M 2006 *Mat. Sci. Eng. B* **133** 167
- [25] Zhang Y-H, Guo L, He L, Liu K, Chen C, Zhang Q and Wu Z 2007 *Nanotechnology* **18** 1
- [26] Nogués J, Sort J, Langlais V, Sukumryev Y, Suriñach S, Muñoz J S and Baró M D 2005 *Phys. Rep.* **422** 65
- [27] Shinohara T, Sato T and Taniyama T 2003 *Phys. Rev. Lett.* **91** 197201
- [28] Liou Y, Su P W and Shen Y L 2007 *Appl. Phys. Letts.* **90** 182508
- [29] Brusetti R, Coey J M D, Czjzek C, Fink J, Gompt R and Schmidt H 1980 *J. Phys. F: Met. Phys.* **10** 33
- [30] Okamura H, Naitoh J, Nanba T, Matoba M, Nishioka M, Anzai S, Shimoyama I, Fukui K, Miura H, Nakagawa H, Nakagawa K and Kinoshita T 1999 *Solid State Commun.* **112** 91
- [31] Kravtsova A N, Stekhin I E, Soldatov A V, Fleet M E and Harmer S L 2004 *J. Phys.: Condens. Matter* **16** 7545
- [32] Chambers S A 2006 *Surf. Sci. Rep.* **61** 345 and references therein